Photochemical and Photophysical Studies of Tetranuclear Copper(I) Halide Clusters: an Overview

Peter C. Ford

Department of Chemistry, University of California, Santa Barbara, CA 93106 USA

ABSTRACT

This presentation will summarize recent studies in these laboratories of the rich luminescence and photoredox properties of tetranuclear copper(I) clusters of the type $Cu_4X_4L_4$.

INTRODUCTION

In combination with various anionic and neutral ligands, d^{10} metal ions form numerous luminescent polynuclear compounds [1]. Prominent examples are cuprous iodide clusters such as $Cu_4I_4py_4$ (I, Fig. 1) [2] which

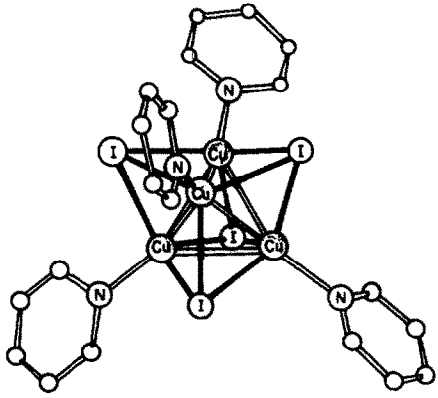

Figure 1: The structure of the $Cu_4I_4py_4$ cluster **I**, redrawn using the ChemX molecular modelling program from the Cambridge data base [2]

display bright emissions with colors markedly dependent on T, a property once termed "luminescence thermochromism" [3]. For **I**, this behavior can be attributed to the presence of two, poorly coupled excited states of different orbital parentages. At ambient temperature, these emissions are an intense band at λ_{max} = 690 nm and a much weaker band at 490 nm in

0010-8545/94/$26.00
SSDI 0010-8545 (94) 02015–B

toluene solution (Fig.2) [4, 5]. Both the intensities and positions of these bands are quite sensitive to the medium and (especially) to the temperature. Summarized here will be experimental and theoretical studies of this and related tetranuclear Cu(I) clusters carried out with the goal of elucidating the relevant excited state (ES) characters. Also described will be kinetics studies of the electron and energy transfer quenching of emission from **I** by a series of tris(β-dionato)chromium(III) complexes and several organic oxidants [6].

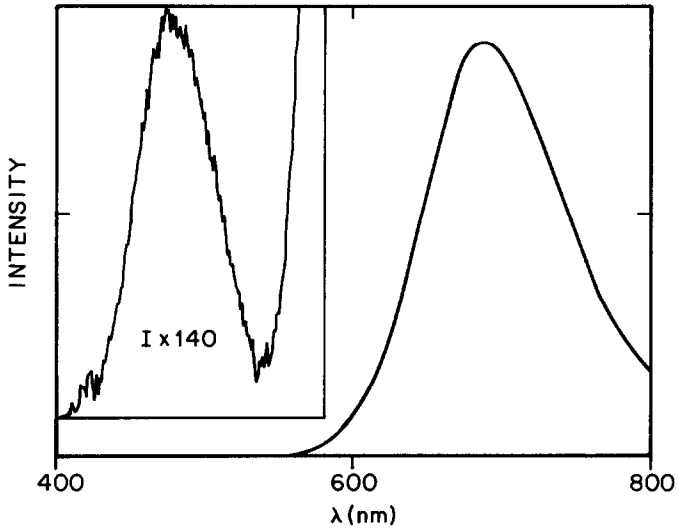

Figure 2: Emission and absorption spectra of the copper(I) cluster $Cu_4I_4(py)_4$ (**I**) in ambient temperature toluene solution. [3]

LUMINESCENCE PROPERTIES OF $Cu_4I_4(py\text{-}x)_4$

The rich luminescence properties of the $Cu_4X_4L_4$ clusters are illustrated by the emission spectrum in Figure 2. At ambient temperature two emissions can be detected, an intense lower energy (LE) band at λ_{max} = 690 nm and a much weaker, higher energy (HE) band at 490 nm [4, 5]. The poor coupling between the two relevant excited states is indicated by the different emission lifetimes (τ), 10.6 μs and 0.45 μs, respectively. Upon lowering T, the LE band first shifts to the red, then sharply to the blue when the solution passes the glass transition. Simultaneously, the HE band, hardly discernable in the room temperature spectrum, becomes much more prominent (Fig. 3), and its lifetime becomes comparable to that of the LE band. The combined effects are responsible for the "luminescence thermochromism" noted above. Notably, solid **I** is white, dilute solutions of **I** are colorless, and the absorption spectrum shows no significant absorbance above 400 nm. UV absorptions increase towards shorter wavelength with strong bands below 300 nm due to the presence of iodide

and pyridine. Diffuse reflectance spectra display weak transitions in the 300-400 nm region. Similarly, the excitation spectra also demonstrate the presence of absorptions in this region.

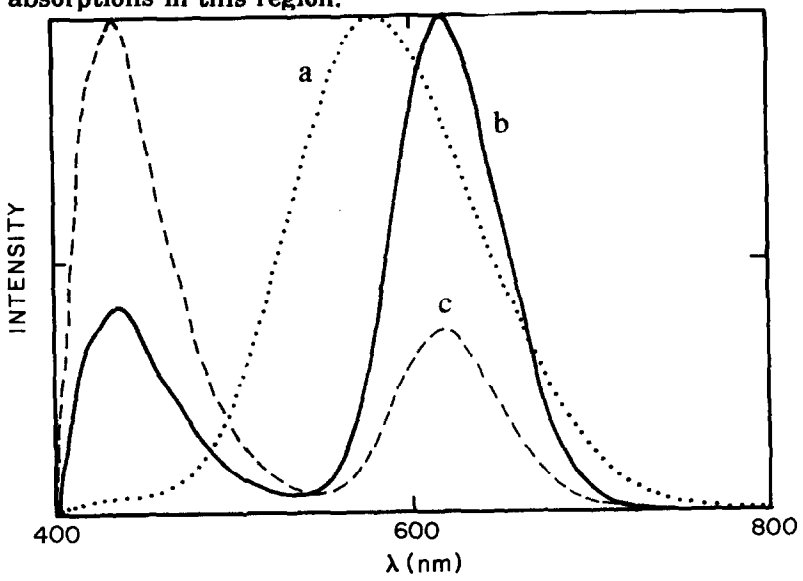

Figure 3. Temperature dependence of normalized solid state spectrum of **I**. a. Spectrum at 295 K (λ^{ex} = 380 nm). b. Spectrum at 77K (λ^{ex} = 330 nm). c. Spectrum at 77K (λ^{ex} = 365 nm).

A key experiment by Vogler and Kunkely [7] showed that the bright LE emission band of I is mimicked by the luminescence spectrum of the saturated amine analog Cu_4I_4(morpholine)$_4$ (II) (λ_{max} 671 nm in toluene). Thus, π-unsaturated ligand orbitals are not involved in this emission, and a metal to ligand charge transfer (MLCT) excited state assignment can be excluded in this case. Instead these workers proposed that a d←s transition was responsible for the emission. Subsequent studies in our laboratories [4] demonstrated that the two bands seen for the emission spectra of I are also present for other Cu_4I_4(py-x)$_4$ (py-x = substituted pyridine), while only the more intense LE emission was seen for II and other saturated amine clusters $Cu_4I_4L_4$. The LE band position proved to be independent of the pyridine substituents, but the HE band to be red-shifted by electron withdrawing substituents (Table 1). Thus, we initially assigned the latter to be emission from a MLCT (d→π^*) excited state [3a] and the LE band to result from a delocalized cluster centered (CC) excited state of d-s character analogous to the assignment by Vogler [7]. The emission lifetimes (Table I) are consistent with a triplet assignment for both emissive states.

The excitation spectrum of I displays different maxima (λ^{ex}) depending on whether the LE or HE emission maximum is the monitoring

wavelength. Interestingly, the λ^{ex} for the so-called HE band occurs at lower energy than does that for the LE emission (Table I), thus the Stokes shift for the latter (1.64 μm^{-1}) is much greater than that for the former (0.77 μm^{-1}). As noted above, the independent lifetimes (Table I) further indicate the relatively uncoupled behavior of the two emission bands for I and related complexes. In solution, the LE emission is the longer lived for various $Cu_4I_4(py\text{-}x)_4$, although lifetime differences are much less at temperatures below the solution glass transition. While observation of two uncoupled emissions from the same compound may lead one to suspect the possible presence of two luminescence active molecular components in such solutions, the close analogies between the photophysical properties of the $Cu_4I_4L_4$ clusters in solution and those of crystallographically well-characterized solids argues strongly for the integrity of these molecular properties [5].

TABLE 1 Photophysical Properties of Representative $Cu_4I_4L_4$ Clusters in Toluene Solution (except where noted)[a,b,c].

		HE			LE		
L	T(K)	λ_{max}	λ^{ex}	τ	λ_{max}	λ^{ex}	τ
pyridine	294	480	352	0.45	690	325	10.6
	77	436	350	32.9	583	317	26.5
solid	77	438	365	23.2	619	330	25.5
4-*t*- butylpy	294	468		0.35	696		10.3
	77	434		38.7	595		43.5
solid	77	437	362	29.2	650	327	38.8
4-benzylpy	294	473		0.56	692		11.0
4-phenylpy	294	520		0.12	694		9.4
3-chloropy	294	537		0.35	675		12.7
piperidine	294	---			680		0.11
morpholine	294	---			671		0.51
	77	---			630		19.8

[a] λ in nm, τ in μs. [b] Data from ref. 5. [c] λ_{max} is emission maximum, λ^{ex} is excitation maximum for that band

Our initial assignments for the emissions from I were subsequently challenged by preliminary *ab initio* calculations in this laboratory which indicated the highest occupied molecular orbitals in both I and $Cu_4I_4(NH_3)_4$ (a model for II) to be composed largely of iodide p-orbitals [8]. Thus, major

contributions of iodide-to-metal charge transfer (XMCT) and iodide-to-ligand charge transfer (XLCT) character to the excited states responsible for the LE and HE emissions, respectively, must be considered. More thorough calculations, taking electronic reorganization into account [9], have subsequently led to our conclusion that the LE emission is occurring from a state of mixed character delocalized over the Cu_4I_4 core with roughly equal contributions from d-s and XMCT components. Thus, the terminology we first offered, i.e. that this state is "cluster centered" (CC), appears to be an apt description.

The very large Stokes shift for the LE band of the $Cu_4I_4(py\text{-}x)_4$ complexes and the corresponding emission band of other $Cu_4I_4L_4$ is consistent with the mixed d-s/XMCT assignment for the CC excited state. Qualitatively, population of 4s-orbitals delocalized over the Cu_4 core should lead to enhanced Cu-Cu bonding. This argument is supported by the results of the *ab initio* calculations [9], which also indicate lessened Cu-I bonding. Hence, the structure of this ES should be significantly distorted from that of the ground state. An analogy can be drawn to the square planar d^8 complexes in face to face arrangements, such as the dinuclear $Pt_2(P_2O_5H_2)_4^{4-}$ species, for which excitation of the $\sigma^* \rightarrow \sigma^b$ transitions leads to markedly enhanced metal-metal bonding in the ES [10]. In contrast, the calculations [9] suggest that much less distortion should be expected for the XLCT states of the $Cu_4I_4(py\text{-}x)_4$ clusters, consistent with the much smaller Stokes shifts seen for the HE emissions. Lastly, distortions of the XLCT state would be along coordinates different from the distortion coordinates of a d-s/XMCT cluster centered ES. Thus, we propose that it is *these differences in the magnitude and direction of the respective distortion coordinates which lead to the poor coupling between the two excited states.*

LUMINESCENCE OF OTHER HALIDE CLUSTERS $Cu_4X_4L_4$:

With the analogous chloride clusters, $Cu_4Cl_4L_4$, emissions were observed only when L is an unsaturated nitrogen heterocycle having empty low-energy π^* orbitals [11]. Accordingly, this type of emission appears to originate from a XLCT or MLCT excited state, the XLCT assignment being favored by the results of *ab initio* calculations which continue to show the HOMO as being predominantly composed of halide orbitals [12]. The absence of a d-s/XMCT cluster centered emission similar to the LE emission seen for the iodide clusters I and II would be consistent with arguments [13] that such emissions are found only for clusters with Cu-Cu distances ($d_{Cu\text{-}Cu}$) less than the sum of the Cu(I) van der Waals radii (2.8 Å). For I and II, these distances are less than 2.7 Å; in contrast, $d_{Cu\text{-}Cu}$ values exceeding 3.0 Å are typical for analogous chloride clusters. The empirical requirement of a short $d_{Cu\text{-}Cu}$ can be attributed to the nature of the acceptor orbitals in the cluster centered state. The intermetallic

interactions of these s-orbitals are Cu-Cu bonding, thus the excited state potential energy surface must be strongly dependent on d_{Cu-Cu}.

In this context, a particularly interesting homologous $Cu_4X_4L_4$ (X = Cl, Br and I) series is one based on the 2-(diphenylmethyl)pyridine ligand (dpmp). The structures of the isomorphous $Cu_4X_4(dpmp)_4$ solids have been determined, and the average d_{Cu-Cu} values are nearly the same (~2.90 Å) for all three clusters [14]. Thus, one can compare the properties of homologous chloride, bromide, and iodide clusters without having to account for major variation of the molecular or crystal structures. The emission spectra of these three solids were examined in this laboratory [15]. At 77 K, all three (as well as glasses of acetonitrile solutions) each display a single XLCT band as the dominant feature in the luminescence spectra (Fig. 4). There is very little difference in the energies of the three emission bands or of their excitation spectra, although the emission energies do follow the order I > Br > Cl. This order seems counter-intuitive to the XLCT assignment given the normal expectation that ionization energies of halide anions increase across the series $I^- \rightarrow Cl^-$. However, *ab initio* calculations [12] show that the halide ionicity in the ground state clusters also increases over the same series owing to the increasing electronegativity. Since IE decreases with increasing ionicity, this compensates for the effects of ionization energy on the (largely halide p-orbital) cluster HOMO's.

When the luminescence of the iodo and bromo $Cu_4X_4(dpmp)_4$ solids were investigated at higher temperature, the spectra displayed a second feature, a long wavelength shoulder (Fig. 5) [15]. This we attribute to a

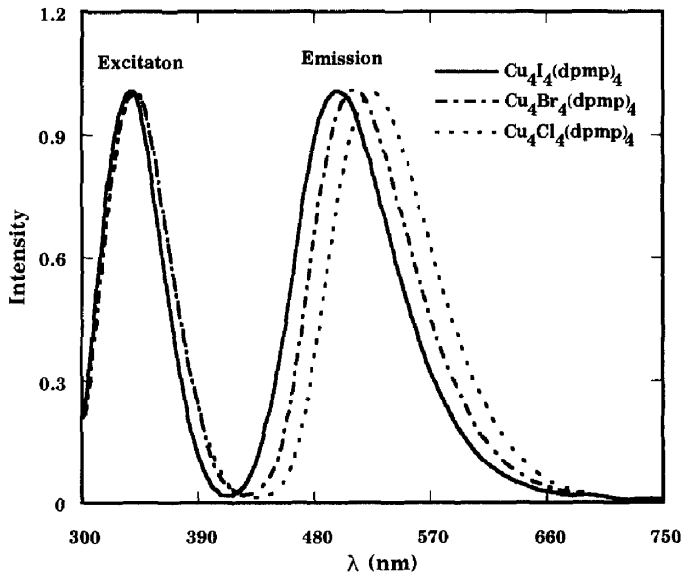

Figure 4: Emission and excitation spectra of $Cu_4X_4(dpmp)_4$ clusters in acetonitrile solution at 77 K

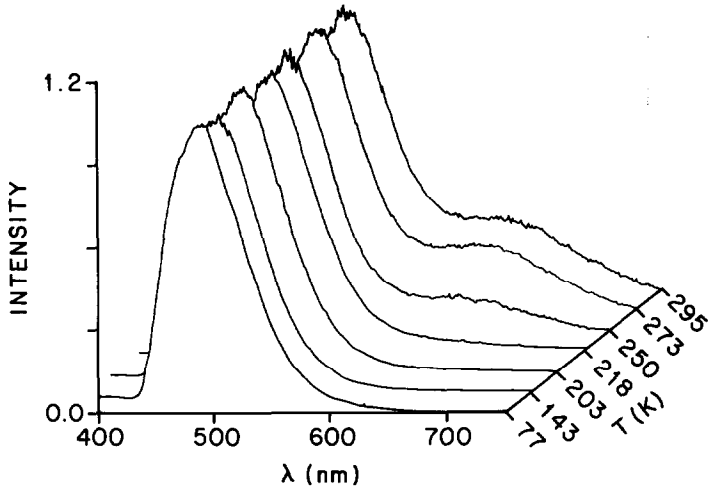

Figure 5: Temperature dependence of emission spectrum of solid $Cu_4Br_4(dpmp)_4$ (380 nm excitation)

thermally promoted cluster centered emission. The intensity of this band increases with T, but the lifetime remains the same as that of the much stronger XLCT emission at the same T. Thus, in contrast to I, the d-s-/XMCT and XLCT states for the dpmp clusters are in thermal equilibrium, with the former occurring at slightly higher energy ($\sim 10^3$ cm^{-1} for $Cu_4Br_4(dpmp)_4$).

In this context, the qualitative energy diagrams indicated in Figure 6 are used to propose a model for the emitting excited states of the clusters $Cu_4I_4py_4$ and $Cu_4X_4(dpmp)_4$. The poor coupling between the XLCT and the cluster centered d-s/XMCT excited states of I is attributed to a high curve-crossing barrier, so that once the molecule is prepared in either state, internal conversion would be slow relative to other photophysical processes. For the dpmp clusters, the CC state is somewhat above the XLCT state, and the barrier height must be small since the two states are coupled at all T. The origin of these differences apparently lies with the $d_{Cu\text{-}Cu}$ distances of the Cu_4 cores. In the cluster centered d-s/XMCT excited state, electron density has been transferred into the $\sigma_{MM}{}^b$ s-orbitals; thus, the energy and shape of this state's potential surface depend strongly on the extent of Cu-Cu interaction. By contrast, the XLCT emissions are little affected by $d_{Cu\text{-}Cu}$. The packing of large iodide and smaller Cu(I) spheres in I and II gives relatively small Cu_4 tetrahedra with greater overlap between relevant metal orbitals. Packing with the chlorides tends to give larger Cu_4 tetrahedra with less Cu-Cu interaction, a result which may explain the failure to observe the cluster centered emission for $Cu_4Cl_4py_4$ or $Cu_4Cl_4(Et_3N)_4$. For the dpmp clusters, the packing in the Cu_4X_4 core appears to be influenced by the steric bulk of the 2-(diphenylmethyl)-

pyridine ligand, and the d_{Cu-Cu} for all three are held at ~2.9 Å. For these complexes, the Cu-Cu interactions are apparently strong enough to give a CC excited state energy above but close to that of the XLCT state from which the emission is principally observed.

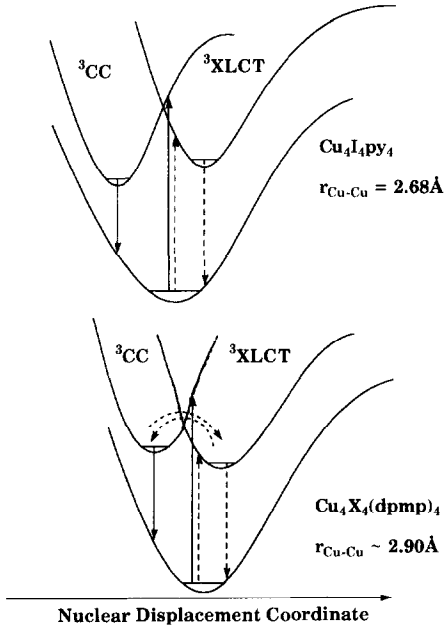

Figure 6: Proposed model for potential energy surfaces for the XLCT and CC (d-s/XMCT) excited state in Cu_4 clusters: Top: $Cu_4I_4py_4$. Bottom: $Cu_4I_4(dpmp)_4$

BIOMOLECULAR EXCITED STATE PROCESSSES OF $Cu_4I_4py_4$

Photochemical studies of Cu(I) clusters are limited by the inherent lability of the ground states, the structures and configurations of which are thermodynamically controlled. Thus, photoreactions as ligand labilization or cluster fragmentation would be rapidly reversible and observable only by flash photolysis. On the other hand, the long luminescence lifetimes in fluid solutions should allow observation of bimolecular processes such as energy or electron transfer to the appropriate receptor, e.g.,.

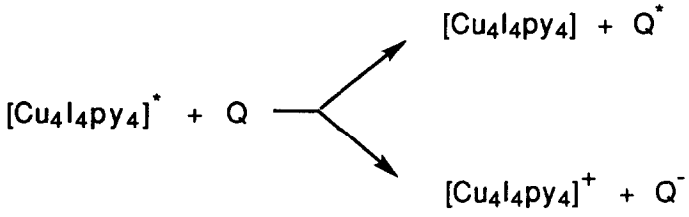

The hypothetical half cell potential for the cluster centered excited state of $Cu_4I_4py_4$ (i.e., for $I^+ + e^- \rightarrow I^{*)}$ was estimated [6] by subtracting the calculated ES energy E^{oo} from the ground state reduction potential , i.e.,

$$E_{1/2}(I^+/I^*) = E_{1/2}(I^+/I) - E^{oo}$$

Cyclic voltammetry measurements gave an approximate value of ~0.28 V for $E_{1/2}(I^+/I)$ vs Fc^+/Fc and the E^{oo} value for the CC state was estimated conservatively as 1.66 μm^{-1} (2.06 V) based upon the "10% rule", namely that the E^{oo} can be estimated as that frequency where an emission band has an intensity 10% that found at the λ_{max}. For a gaussian band this can be calculated from the formula $E^{oo} = \nu_{max} + 0.91\ \nu_{1/2}$, where ν_{max} is the energy of the band maximum and $\nu_{1/2}$ is the full width at half-maximum. On this basis a $E_{1/2}(I^+/I^*)$ value of -1.78 V was estimated

The emission from I^* can be quenched by a series of uncharged tris(β-dionato)chromium(III) complexes CrL_3 [6]. These quenchers display a remarkable range of reduction potentials ($E_{1/2}$ =-2.51 V to -0.87 V vs Fc^+/Fc in CH_2Cl_2) but have lowest ES energies (1.22-1.28 μm^{-1} independent of the ligand substituents) below the estimated E^{oo} of the LE state [16, 17]. Thus each CrL_3 can quench I^* by energy transfer, and, indeed, k_q values of ~4.6 x 10^7 M^{-1} s^{-1} are seen for those CrL_3 which do not have reductions potentials sufficiently large to quench by electron transfer. Those with the least negative $E_{1/2}(Q/Q^-)$ values may also quench I^* by competitive electron transfer (eq. 1), and k_q values approaching diffusion limits in these cases suggest contributions from such a pathway. This behavior is illustrated in Fig. 7.

Quenching of I^* was also seen for a series of nitroaromatic organic oxidants which have $\pi\pi^*$ state energies too high for energy transfer to be viable (>1.74 μm^{-1}) and have $E_{1/2}(Q/Q^-)$ values in the range of -1.37 V to -0.94 V vs ferrocene [6]. Table 2 lists some representative results. Substantially negative ΔG_{el}^o (free energy change of the ES electron transfer process) values are required for electron transfer quenching of I^* to be competitive with radiative and nonradiative deactivation (Fig. 7). This suggests that electron transfer from the d-s/XMCT cluster centered state is unusually slow, perhaps because the enhanced Cu-Cu bonding in I^* lends a large inner sphere contribution to the total reorganization energy accompanying the electron transfer. This may also explain the substantial $\Delta H^{\ddagger}$ values for several of these quenchers. In contrast, there was little temperature dependence on the rates of quenching by the CrL_3 complexes which must operate by energy transfer alone.

Pressure effects on the energy/electron transfer quenching of I^* were also examined. These can be qualitatively separated into three regimes. For k_q values approaching the diffusion limit, pressure decreased k_q ($\Delta V^{\ddagger}$ values were positive) owing to pressure induced changes in diffusion rates.

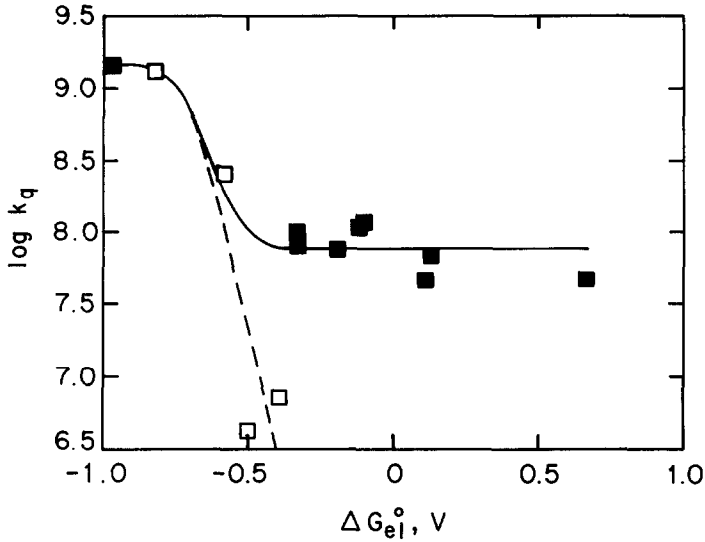

Figure 7: Plot of log (k_q) vs the free energy of electron transfer ΔG_{el}^{0}. Filled and open squares represent experimental data for CrL_3 and organic quenchers, respectively. The dotted and the solid curve represent least squares fits to the equation $1/k_q = 1/k_d + 1/k_Q$, where $k_Q = (k_{el} + k_{en})(k_d/k_{-d})$, with k_{el} estimated according to the Marcus Cross relation and k_{en} equals 0 for aromatic oxidants and an ave. value of $10^{7.8}$ M^{-1} s^{-1} for the CrL_3 quenchers as described in ref. 6.

Table 2.: Rate Constants and Activation Parameters for Quenching of I* by Various Quenchers (data from ref. 6).

Quencher[a]	$-E_{1/2}$[b] (V)	ΔG_{et}^{o} (V)[c]	10^{-7} k_q[d] ($M^{-1}s^{-1}$)	$\Delta H_q^{\ddagger}$ kJ mol^{-1}	$\Delta V_q^{\ddagger}$ cm^3 mol^{-1}
$Cr(acac)_3$	2.43	0.65	4.7	0.5	-0.3
$Cr(dbm)_3$	1.87	0.09	4.6		
$Cr(tfac)_3$	1.64	-0.14	10.9		
$Cr(tta)_3$	1.43	-0.35	8.1		
$Cr(tfbzac)_3$	1.43	-0.35	10.0	0.7	+0.2
$Cr(hfac)_3$	0.79	-0.99	141.	1.1	+6.6
m-dinitro-benzene	1.37	-0.41	0.72	28	-8.2
o-dinitrobenzene	1.26	-0.52	0.42	40	-7.0
p-dinitrobenzene	1.18	-0.60	25.3		
1,4-benzo-quinone	0.94	-0.84	129.	5.4	+5.2

[a] ligand abbreviations: acac = 2,4-pentanedionate (acetylacetonate); dbm = 1,3-diphenyl-1,3-propanedionate; hfac = 1,1,1,5,5,5-hexafluoro-2,4-pentanedionate; tfac = 1,1,1-trifluoro-2,4-pentanedionate; tta = 4,4,4-trifluoro-1-(2-thienyl)-1,3-butanedionate; tfbzac = 4,4,4-trifluoro-1-phenyl-1,3-butanedionate. [b] Reduction potential vs ferrocenium/ferrocene in CH_2Cl_2 (from ref. 6). [c] Free energy of the electron transfer reaction $I^* + Q = I^+ + Q^-$, [d] Second order quenching constant from Stern-Volmer plots.

For quenchers with very negative $E_{1/2}(Q/Q^-)$ values (i.e. those which must operate by an energy transfer mechanism) $\Delta V^{\ddagger}$ is nearly zero. However, those for which electron transfer is less than diffusion limited and is competitive with energy transfer, substantially negative $\Delta V^{\ddagger}$ values were seen. These would appear to reflect the substantial outer sphere solvent reorganization energy resulting from the charge separation accompanying electron transfer between I^* and Q to give I^+ plus Q^-.

SUMMARY

A number of the copper(I) tetrahedral clusters are brightly luminescent, and these often show strongly medium and temperature dependent spectral profiles. Emissions from the iodo species $Cu_4I_4L_4$ (L = py or pip) and some related complexes have been assigned to "cluster centered' state (of mixed d-s/XMCT character) which involve a resistribution of charge within the Cu_4I_4 core. A key feature of such a CC state is enhanced electronic population of metal-metal bonding orbitals in these states as evidenced by the large Stokes shifts between excitation and emission maxima. Such emission bands is strongly favored by relatively short Cu-Cu distances in the clusters. With π–unsaturated ligands L, emissions from XLCT excited states of $Cu_4X_4L_4$ are also observed, and the luminescence thermochromism of such complexes is the result of different temperature and medium rigidity responses of the two types of excited states. The poor coupling between the CC and XLCT states in compounds such as $Cu_4I_4py_4$ can be attributed to high barrier heights for curve crossing owing to different distortion trajectories once the molecule is prepared in one of the respective excited states. This large distortion may also explain the relatively large reorganization energies noted for electron transfer from the CC state of $Cu_4I_4py_4$.

ACKNOWLEDGEMENT

This work was supported by the United States National Science Foundation (Grants No. CHE-8722561 and CHE-9024845) (PCF). The following coworkers at UC Santa Barbara contributed significantly to the studies described in this article: Dr. Kevin Kyle, Dr. Chong K. Ryu, Dr. Marcello Vitale, Dr. Anders Dϕssing, Prof. W. E. Palke, Dr. S. Kudo.

REFERENCES:

1. Ford,. P. C.; Vogler, A. *Accts Chem. Res.* **1993**, *26*, 220-226
2. Raston, C. L.; White, A. H. *J. Chem. Soc., Dalton Trans.* **1976**, 2153-2156
3. (a) De Ahna, H. D.; Hardt, H. D. *Z. Anorg. Allg. Chem.* **1972**, *387*, 61; (b) Hardt, H. D. Gechnizdjani, H. *Z. Anorg. Allg. Chem.* **1973**, *397*, 23; (c) Hardt, H. D.; Pierre, A. *Z. Anorg. Allg. Chem.* **1973**, *402*, 107; (d) Hardt, H. D.; Pierre, A. *Inorg. Chim. Acta* **1977**, *25*, L59; (e) Hardt, H. D.; Stoll, H.-J. *Z. Anorg. Allg. Chem.* **1981**, *480*, 193; (f) Hardt, H. D.; Stoll, H.-J. *Z. Anorg. Allg. Chem.* **1981**, *480*, 199.
4. (a) Kyle, K. R.; DiBenedetto, J.; Ford, P. C. *J. Chem. Soc. Chem. Commun.* **1989**, 714. (b) Kyle, K. R.; Ford, P. C. *J. Am. Chem. Soc.* **1989**, *111*, 5005.
5. Kyle, K. R.; Ryu, C. K.; Ford, P C. *J. Am. Chem. Soc.* **1991**, *113*, 2954.
6. Dóssing,A.; Ryu, C. K.,Kudo, S.; Ford, P. C. *J. Am. Chem. Soc.* **1993**, *115*, 5132-5137.
7. Vogler, A.; Kunkely, H. *J. Am. Chem. Soc.* **1986**, *108*, 7211.
8. Kyle, K. R.; Palke, W .E.; Ford, P C. *Coord. Chem. Rev.* **1990**, *97*, 35-46
9. Vitale, M.; Palke, W. E.; Ford, P. C. *J. Phys. Chem.* **1992**, *96*, 8329-8336
10. Roundhill, D. M.; Gray, H. B.; Che, C.-M. *Acc. Chem. Res.* **1989**, *22*, 55.
11. Ryu, C. K.; Kyle, K. R.; Ford, P. C. *Inorg. Chem.*, **1991**, *30*, 3982-3986
12. Vitale, M., Ph.D. Dissertation, UC Santa Barbara, 1993
13. (a) Rath, N. P.; Holt, E. M.; Tanimura, K. *Inorg. Chem.* **1985**, *24*, 3934; (b) Rath, N. P.; Holt, E. M.; Tanimura, K. *J. Chem. Soc., Dalton Trans.* **1986**, 2303; (c) Rath, N. P.; Maxwell, J. L.; Holt, E. M. *J. Chem. Soc. Dalton Trans.* **1986**, 2449; (d) Tompkins, J. A.; Maxwell, J. L.; Holt, E. M. *Inorg. Chim. Acta* **1987**, *127*, 1.
14. Engelhardt, L. M.; Healy, P. C.; Kildea, J. D.; White, A. H. *Aust. J. Chem.* **1989**, *42*, 107-113.
15. Ryu, C. K.; Vitale, M..; Ford, P. C., *Inorg. Chem.*, **1993** *32*,869-874
16. Gamache, R. E., Jr.; Rader, R. A.; McMillin, D. R. *J. Am. Chem. Soc.* **1985**, *107*, 1141-1146.
17. (a) Crane, D. R.; Ford, P. C. *J. Am. Chem. Soc.* **1991**, *113*, 8510-8516. (b) Crane, D. R.; Ford, P. C. *Inorg Chem.* **1993**, *32*, 2391-2393